Open access • Journal Article • DOI:10.1063/1.3369450

Thermal stability of copper nitride thin films: The role of nitrogen migration

Raquel González-Arrabal, N. Gordillo, Marisol Martín-González, R. Ruiz-Bustos ...+1 more authors

Published on: 20 May 2010 - Journal of Applied Physics (American Institute of Physics)

Topics: Nitride, Thin film, Solid solution, Crystal structure and X-ray crystallography

Thermal stability of copper nitride thin films: The role of nitrogen migration

R. Gonzalez-Arrabal,[1,2,a)] N. Gordillo,[3,4] M. S. Martin-Gonzalez,[2] R. Ruiz-Bustos,[5] and F. Agulló-López[4,6]

[1]*Instituto de Fusión Nuclear, ETSI de Industriales, Universidad Politécnica de Madrid, E-28006 Madrid, Spain*
[2]*Instituto de Microelectrónica de Madrid, C/Isaac Newton, 8 Tres Cantos, E-28760 Madrid, Spain*
[3]*Parque Científico de Madrid, Campus de Cantoblanco, E-28049 Madrid, Spain*
[4]*Centro de Microanálisis de Materiales, Universidad Autónoma de Madrid, E-28049 Madrid, Spain*
[5]*Instituto de Energías Renovables, Parque Científico y Tecnológico de Albacete, Paseo de la Investigación 1, E-02006 Albacete, Spain*
[6]*Departamento de Física de Materiales, Universidad Autónoma de Madrid, E-28049 Madrid, Spain*

(Received 6 October 2009; accepted 22 February 2010; published online 20 May 2010)

The atomic composition, structural, morphological, and optical properties of N-rich copper nitride thin films have been investigated prior to and after annealing them in vacuum at temperatures up to 300 °C. Films were characterized by means of ion-beam analysis (IBMA), X-ray diffraction (XRD), atomic force microscopy (AFM), and spectroscopic ellipsometry techniques (SE). The data reveal that even when the total (integrated over the whole thickness) atomic composition of the films remains constant, nitrogen starts to migrate from the bulk to the film surface, without out-diffusing, at temperatures as low as 100 °C. This migration leads to two chemical phases with different atomic concentration of nitrogen, lattice parameters, and crystallographic orientation but with the same crystal structure. XRD experimental and Rietveld refined data seem to confirm that nitrogen excess accommodates in interstitial locations within the anti-ReO_3 crystal lattice forming a solid solution. The influence of nitrogen migration on the optical (electronic) properties of the films will be discussed. © *2010 American Institute of Physics*. [doi:10.1063/1.3369450]

I. INTRODUCTION

Copper nitride is a metastable semiconducting material with a cubic anti-ReO_3 type crystal structure where the face-centered-cubic close-packed sites are vacant. Since the pioneer work by Terada *et al.*[1] different methods have been applied to grow films with reasonable quality: molecular beam epitaxy,[2] atomic layer deposition,[3] pulsed laser deposition,[4,5] dc-triode sputtering,[6,7] and mostly rf-magnetron sputtering.[8–14]

Copper nitride decomposes at relatively low temperature into metallic copper and nitrogen. This process can also be induced by irradiation with electrons and laser pulses. The radiation-induced decomposition of the material opens the possibility to use it for write-once optical data storage with a strong reflectivity contrast which allows for writing rates above 3 Mbits/s. Moreover, maskless laser writing enables the production of micrometric conductive dot and line patterns[15] having a signal speed higher than those based on Al, currently used in integrated circuits. Finally, Cu_3N has been also suggested to be used as a barrier material in tunnel junctions,[16] as a substrate for the growth of single-crystals of porphyrins and of atomic nanowires[17] and as a good candidate for hybrid inorganic-organic solar cells.[2]

From a fundamental point of view the family of Cu–N compounds offers a rich variety of electronic properties depending on chemical composition, ranging from fully metallic (Cu_4N) (Ref. 18) to semiconducting (Cu_3N) behavior. In fact, as in many other nitrides[19–21] the film stoichiometry can be tuned from nitrogen deficient to nitrogen rich, by changing deposition conditions.[6–8]

The thermal stability of copper nitride films is a key problem for exploiting their technological potential and assuring their industrial implementation. Some studies performed so far on the thermal properties of these films have been focused on their decomposition temperature[11,22,23] whose reported values show a large dispersion from 100 (Ref. 11) to 450 °C.[15] Nevertheless, as far as we know, the physical mechanisms involved in the decomposition process have not been sufficiently investigated and, therefore, many questions remain still open. Does nitrogen diffuse when increasing the film temperature? Are new crystal phases generated during the thermal decomposition process? If so, what is the influence of these phases on the physical properties of the material? As it will be shown in this paper most of the questions are essentially related to the binding and migration of the volatile (N) component inside the crystal lattice.

In the particular case of N-rich Cu_3N, the situation is even more complex since we are concerned with the long-standing problem of the extra nitrogen location. Is it at interstitial lattice sites like in other 3*d* metals nitrides[19] or is it trapped at grain boundaries like previously suggested in literature?[13]

The aim of this paper is to systematically investigate the route to the thermal decomposition of N-rich copper nitride films, to unveil the responsible physical processes and to answer some of the previously exposed open questions. For this purpose, the atomic composition, the structural, morphological and optical properties of N-rich Cu_3N films have

a)Author to whom correspondence should be addressed. Electronic mail: raquel.gonzalez.arrabal@upm.es.

been characterized prior to and after annealing them in vacuum in the temperature range from 100 to 300 °C by means of ion-beam analysis , x-ray diffraction, atomic force microscopy, and spectroscopic ellipsometry techniques. The obtained results shed new light into the understanding of the thermal decomposition process and provide evidence that nitrogen gets mobile at temperatures as low as 100 °C. This migration generates a nitrogen concentration gradient and gives rise to two new crystalline phases with well-defined atomic concentrations of nitrogen and lattice parameters. XRD and SE data are consistent with a coherent physical scheme that involves a solid solution of the excess nitrogen occupying definite lattice sites in the Cu_3N structure (possibly cubic center positions).

II. EXPERIMENTAL

Copper nitrides thin films with a thickness of ~100 nm were deposited by dc triode sputtering from a copper commercial target on transmitting glass substrates (~1.1 mm thickness). The deposition was performed in the presence of an $Ar+N_2$ atmosphere at room temperature and at a cathode voltage (DC bias) of −1.0 kV. The total working pressure ($P_{Ar}+P_{N_2}$) and the P_{Ar}/P_{N_2} ratio were 8×10^{-1} Pa and 0.9, respectively. More details about the deposition procedure are found in Ref. 6

The samples were separately annealed at temperatures of 100, 250, and 300 °C under vacuum conditions ($P \leq 10^{-3}$ Pa) for 30 min. After finishing the heat treatments, the films were left to cool-down for 90 min before exposing them to environmental conditions.

IBA techniques, in particular Rutherford and non-Rutherford backscattering spectroscopy (RBS, non-RBS) in combination with nuclear reaction analysis (NRA), were used to determine the elemental chemical composition of the films. RBS and non-RBS measurements were performed at the Centre of Microanalysis of Materials (CMAM/UAM) (Refs. 24 and 25) using a He^+ beam at the energy of 2.00 and 3.70 MeV, respectively. More details about the determination of the nitrogen concentration are described elsewhere.[6,26] Since in both, RBS and non-RBS spectra, the peak associated to nitrogen is mounted on a high background related to the substrate, NRA experiments, using the nuclear reaction $^{14}N(d,\alpha)^{12}C$,[27] were carried out in order to determine the nitrogen concentration in a more accurate way. The experiments were performed at the Institute of Ion Beam Physics and Materials Research (FZD), using a D^+ beam at an energy of 1.80 MeV and an implanted Si detector located at 150° to the beam direction. Absolute values of the atomic concentration of nitrogen were obtained by comparing NRA data for the analyzed films with those of a TiN reference sample. Since no stopper foils in front of the detector were used, the Cu concentration was provided simultaneously by evaluating the area of the peak of backscattered deuterons in the spectra (d_{Cu}).

The beam current densities were kept very low to avoid any heating and/or damaging of the samples. In fact, four IBA spectra were sequentially measured in the same spot and under the same conditions at a fluence higher than the one used for standard analysis in order to assure that the elemental composition does not change neither by He^+ nor by D^+ irradiation.

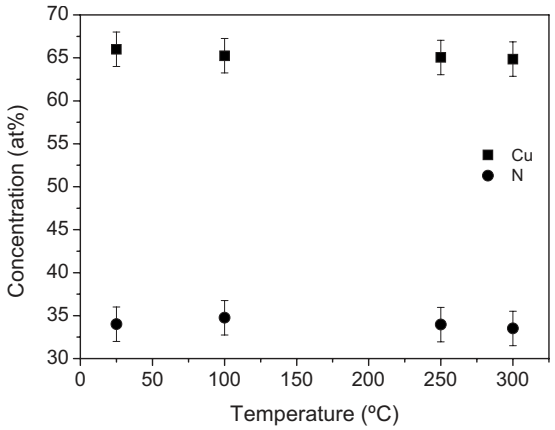

FIG. 1. Total (integrated over the whole sample thickness) concentration of copper (black squares) and nitrogen (black circles) estimated from RBS and NRA data as a function of annealing temperature.

Structural characterization of the films was done by XRD using a diffractometer equipped with a general area detector diffraction system bidimensional detector (Bruker-AXS, model D8 Advanced) a Cu $K\alpha$ radiation source and a collimator of 0.3 mm. XRD measurements were carried out in Debye–Scherrer geometry. Rietveld structural refinements of the XRD data were performed by the general structure analysis system (GSAS) package.[28]

The morphology of the film surface was imaged by a commercial Nanotec Electronics S.L. AFM operated in the dynamic mode. A Si tip of 20 nm of diameter and typical frequency around 60–70 kHz, special for dynamic mode was used. Topography data were analyzed by the software WSXM, from Nanotec Electronics S.L.[29]

The optical characterization of the film was carried out with a Woollam ellipsometer at room temperature in the wavelength range from 350 to 1800 nm at an incidence angle of 70°.

III. RESULTS AND DISCUSSION

A. Atomic composition

The overall (integrated over the whole film thickness) atomic concentration of copper and nitrogen determined from RBS and NRA spectra are shown in Fig. 1. For the as-deposited films the calculated N concentration is 33 ± 2 at. %, corresponding to N-rich films. It is observed that the overall concentration of copper (black squares) and of nitrogen (black dots) do not significantly change after annealing. This indicates that the average stoichiometry of the films is essentially preserved after vacuum annealing at temperatures up to 300 °C.

Some additional information about the annealing-induced changes can be derived from the shape of the RBS and NRA peaks. The shape of the copper peak (d_{Cu}) in the RBS spectra (not shown) is highly symmetric for both the as-deposited and annealed films, pointing to a homogeneous distribution of copper along the whole sample thickness. On

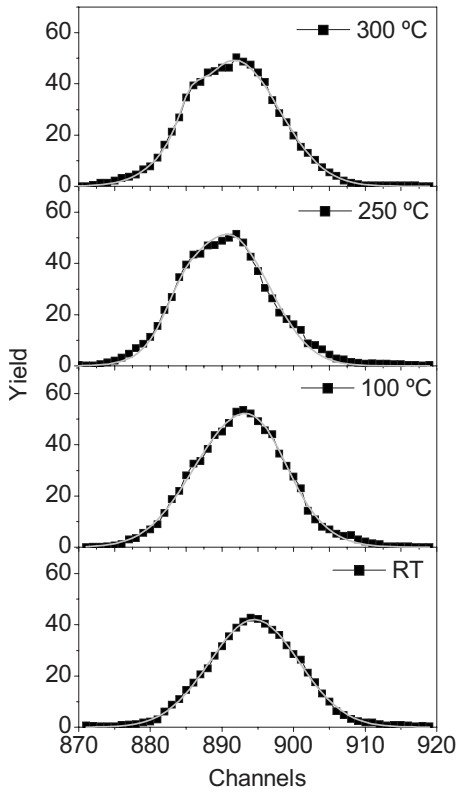

FIG. 2. α_0 peak in the NRA spectra (related to the nitrogen) for as-deposited and heated films as a function of annealing temperature (black points). Gaussian fit of the measured α_0 peaks (gray line).

the other hand, the profiles of the α_1 (not shown) and α_0 (illustrated in Fig. 2) peaks, associated to N are also symmetric before annealing but develop a clear asymmetry with annealing which increases with raising temperature. This asymmetry is a fingerprint of an inhomogeneous nitrogen concentration distribution along the film thickness. In fact, a small jump ($\sim$10–15%) in the NRA yield is clearly observed around the middle depth of the film for annealing temperatures of 250 and 300 °C which indicates an enhancement of the nitrogen concentration in the upper layer of the film. Nevertheless, since the α_0 peak results from a convolution of the true N concentration profile with the resolution function of the detector and they have, both, a comparable width, a precise quantitative analysis from these data is not possible.

It is very interesting to remark that RBS spectra reveal that a Cu–O–N layer, with a thickness of $\sim$6 nm, develops on the film surface when exposing the unprotected samples to environmental conditions. A complementary characterization of this layer has been carried out for similar films by scanning in energy below and above the resonance energy of the $^{16}O(\alpha,\alpha)$ ^{16}O reaction.[30] No oxygen was detected within the films below the surface. The presence of this Cu–O–N surface layer appears to play a relevant role acting as a barrier for N out-diffusion during annealing as further discussed below.

B. Structural characterization

Relevant structural modifications are observed during isothermal annealing as evidenced by the XRD patterns

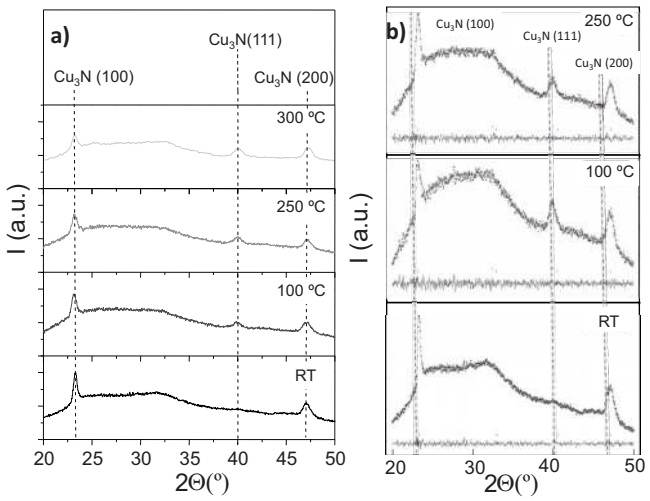

FIG. 3. (Color online) (a) Measured XRD patterns for as-deposited (black line), annealed at 100 °C (dark gray line), at 250 °C (gray line), and at 300 °C (light gray line) N-rich Cu_3N thin films. (b) Measured XRD patterns (black cross), Rietveld refinement calculations (gray line) for three representative films. The gray straight line at the bottom indicates the goodness of the fit.

shown in Fig. 3(a). The as-deposited film exhibits two Bragg peaks, at $2\theta=23.30°$ and $2\theta=47.07°$, which are close to the (100) and (200) reflections reported for stoichiometric Cu_3N.[31] A third additional Bragg peak, located at $2\theta=40.30°$, is observed in XRD patterns for all annealed films. This new peak appears to correspond to the (111) Cu_3N reflection.[31] Other peaks related to pure copper, or to other possible Cu-, or N-compounds are seen, neither for the as-deposited, nor for the annealed layers.

As illustrated in Fig. 3 a clear dependence of the intensity of the XRD peaks on annealing temperature is observed. In general, the intensity of the (100) and (200) peaks decreases with raising temperature, whereas that of the (111) peak increases. This result suggests that annealing favors the (111) orientation over the (100) one.

The structural parameters for as-deposited and selected annealed films are refined by the Rietveld method using the GSAS program package. The model was based on a single-phase anti-ReO_3 structure (space group $Pm3m$). For the as-deposited film a preferential (100) orientation of the grains and an unique lattice parameter equal to 3.892 Å was obtained. On the other hand, the XRD patterns for annealed films can be only well fitted by assuming two different types of crystal grains with lattice parameters of: 3.870 and 3.922 Å oriented along (100) and (111) crystallographic directions, respectively. The fits of the XRD spectra on the basis of the Rietveld refinement method for three representative samples are depicted in Fig. 3(b) and the main characteristics of as-deposited and annealed films are listed in Table I.

These results indicate that the generated nitrogen concentration gradient along the film thickness, together with the temperature reached during the annealing results into two well defined chemical phases. Nevertheless, the reason why these particular phases and no others are formed is uncertain and need to be further investigated. However, it is worthwhile to mention that the preferential orientation of the crystalline grains, either (100) or (111), has been previously re-

TABLE I. rms, Rietveld refined lattice parameters and phase percentages, layer thicknesses, and free carrier densities for as-deposited and annealed N-rich Cu_3N films.

Sample code	rms (nm)	Calculated lattice parameter (Å)		Phase percentage ratio		Thickness (nm)		Free carrier density ($\times 10^{19}$ cm^{-3})	
		a_1	a_2	$Phase_1$	$Phase_2$	Layer 2	Layer 3	Layer 2	Layer 3
As-deposited	0.80	3.892	···	100	···	91	···	4.0	···
RTA-100	0.90	3.870	3.926	66	34	41	70	2.6	0.4
RTA-250	7.00	3.865	3.922	74	26	···	···	···	···
RTA-300	7.00	···	···	···	···	18	98	1.9	···

ported in literature to be strongly dependent on deposition conditions, e.g., substrate temperature,[22] and N partial pressure.[14] Moreover, the ratio of the (100) and (111) diffraction peaks has also been observed to change during annealing treatments.[22] All those data suggest a delicate balance of kinetic and thermodynamical contributions to determine the final texture of the film. While so far an explanation has not been proposed for this behavior, our experiments have shown that the nitrogen concentration gradient coupled to the annealing temperature selects the final texture of the grains within the film.

One possible way to gain inside into the location of extra nitrogen from the XRD data is to plot the available data on lattice parameter (a) versus the nitrogen concentration (c) for a variety of Cu–N compounds (including pure Cu) as plotted in Fig. 4. A clear linear dependence (Vegard law-type) of lattice parameter on atomic concentration of nitrogen is found which is indicative of a homogeneous N–Cu alloy consisting of N atoms occupying noninteracting interstitial sites, very likely the center of the unit cell, in an unique crystal structure. It is also relevant to note that the straight line in Fig. 4 fits the data point corresponding to pure Cu (fcc structure) suggesting that the family of Cu–N compounds may derive from the basic Cu crystal lattice after adding N atoms to certain lattice sites. In particular, as shown in Fig. 5, the Cu_3N unit cell can be build by combining two Cu unit cells, removing Cu atoms from the *ac* face and filling up with N atoms the empty octahedrical positions (NCu_6) in the *ab* face.

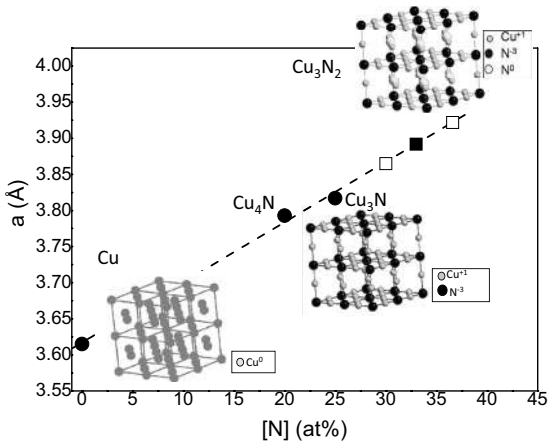

FIG. 4. Lattice parameter as a function of the atomic concentration of nitrogen. In these figure the data corresponding to Cu (Ref. 36), Cu_4N (Ref. 37), and Cu_3N (Ref. 31) crystals (closed circles), have been taken from the Joint Committee for Powder Diffraction Standard database. The other data point (closed square) stands for the value obtained in this and in a previous (Ref. 6) publication for N-rich Cu_3N films containing 33 ± 2 at. N%. The open squares are obtained when bringing to the straight line the two refined lattice parameters for annealed films. The accepted crystal structures for the Cu and Cu_3N samples and the one proposed for Cu_3N_2 are also plotted.

C. Morphological characterization

The morphology of the film surfaces was investigated by means of AFM. AFM images of the surface of as-deposited and annealed films are depicted in Fig. 6 (upper picture).

The as-deposited film presents a very flat and uniform surface exhibiting plane areas of $\sim 120 \times 120$ nm^2. The surface root-mean-square roughness (rms) is ~0.70 nm. This value steadily increases when raising annealing temperature. Nevertheless, the surface of the film annealed at 100 °C is still quite flat (rms ~ 0.90 nm) and regular. For layers annealed at temperatures of 250 °C the surface is no more homogeneous but some bumps of nanometer diameters which are randomly distributed start to develop on it. We can speculate that these bumps correspond to bubbles filled with nitrogen gas, in accordance with previous results reported for similar metal nitrides.[32] The bubbles are more clearly visible for the sample annealed at 300 °C right underneath (B) as well as, on the film surface (A) [see Fig. 6(a)]. They present a semispherical-like shape with a diameter of ~100 nm and a height of ~25 nm. As shown in Fig. 6(b) the surface region of this layer free of bubbles is still quite flat presenting a rms of around 3 nm.

One may consider that the bubbles develop as a consequence of nitrogen accumulation and the subsequent formation of molecular N_2 through pairing of N atoms. In order to check the composition of the bubbles micro-Raman experiments were carried out. Unfortunately, we could not observe

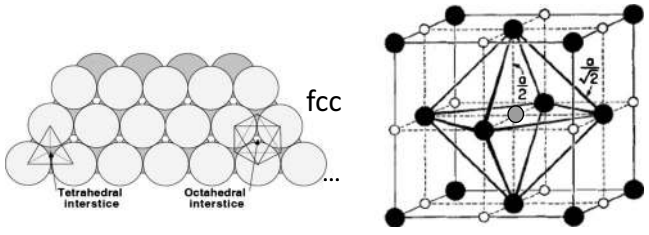

FIG. 5. Schematic picture of fcc pure copper (left side). Formation of the Cu_3N anti-ReO_3 structure from the Cu lattice by combining two Cu unit cells, removing Cu atoms from the *ac* face, and filling up the empty octahedral positions (NCu_6) in the *ab* face (right side) with N atoms.

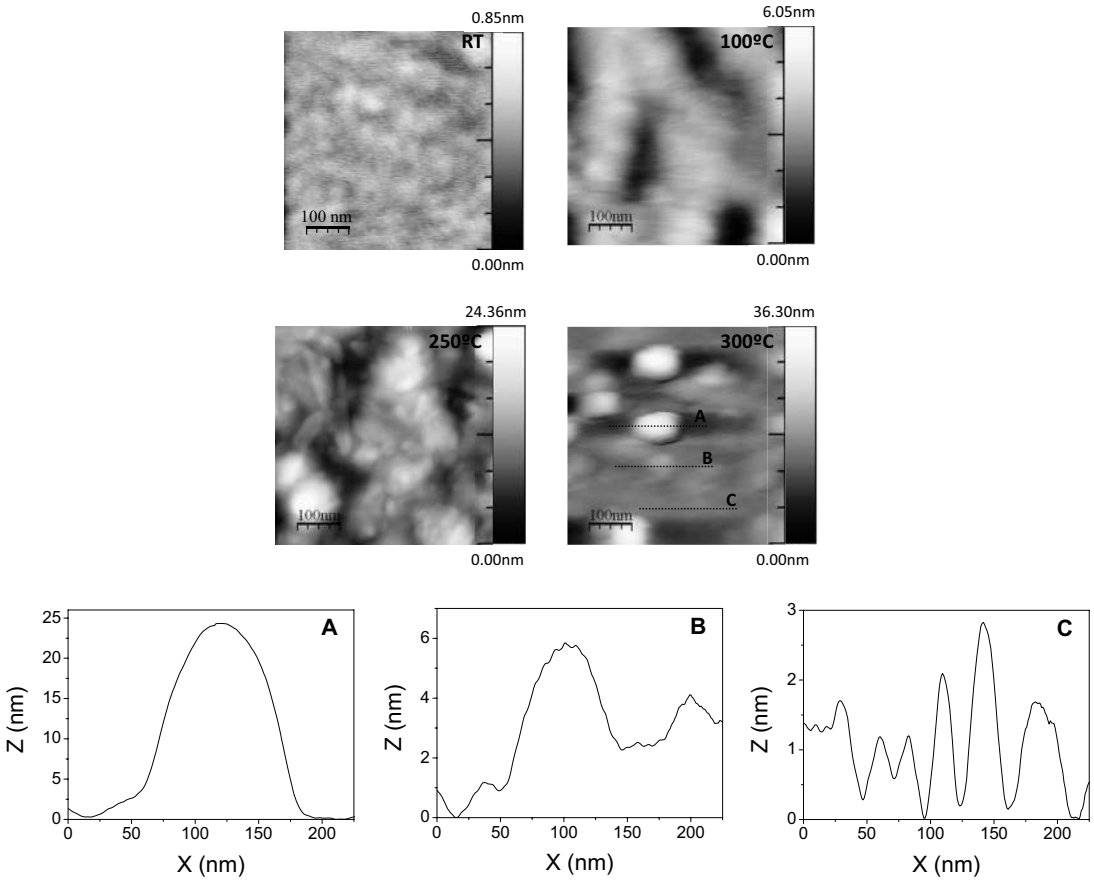

FIG. 6. (a) Surface topography images taken by AFM for as-deposited and annealed at 100, 250, and 300 °C N-rich Cu_3N thin films. (b) Bubbles profiles measured along different regions on sample annealed (300 °C): (a) on the film surface, (b) underneath the surface, and (c) on a flat surface region without bubbles.

any N_2 peak in the Raman spectra, very probably because of the small size of the bubbles and their low nitrogen concentration.

The formation of bubbles may be considered as an experimental evidence for the existence of a nitrogen acceptance limit into the structure. Thus, annealing drives the nitrogen atoms to move from the bulk to the surface layers where it is incorporated into the structure whenever the free energy balance of the system is favorable. However, above a certain nitrogen concentration limit the further incorporation of nitrogen into the structure might increase the free energy of the system becoming an unfavorable process. This assumption is supported by the high formation enthalpy calculated value (4.01 eV/f.u.) for the Cu_3N_2 (Ref. 33) which indicates that the formation of this compound is very unlikely.

The fact that the gas bubbles get trapped underneath and on the sample surface instead of diffusing out of the material can be explained by considering that the Cu–O–N layer formed on the film surface acts as a diffusion barrier as observed for similar nitrides.[34]

A schematic picture for as-deposited and annealed films which summarizes the annealing-promoted layer structures is shown in Fig. 7.

D. Optical characterization

In order to complete the physical picture, the annealing induced changes in the optical properties of N-rich Cu_3N films were characterized by ellipsometry in the 300–1800 nm range at an incidence angle of 70°. The results are shown in Fig. 8. Clear differences are observed indicating that annealing changes the optical properties of the films. In order to get a better insight and to understand the origin of these changes some models have been developed to fit the measured SE data.

For the as-deposited film, as depicted in Fig. 7(a) a three layers model, air (*layer 1*), a N-rich Cu_3N film with a thickness d_2 (*layer 2*) and the glass substrate (*layer 3*) is demonstrated to properly fit the experimental data. This model considers direct optical transitions corresponding to the stoichiometric semiconductor Cu_3N plus a free-carrier (Drude) contribution which can be tuned in accordance with the N-excess. More details about the optical model and the fitting procedure are described in Ref. 35. The calculated layer thickness and their free carrier density are listed in Table I.

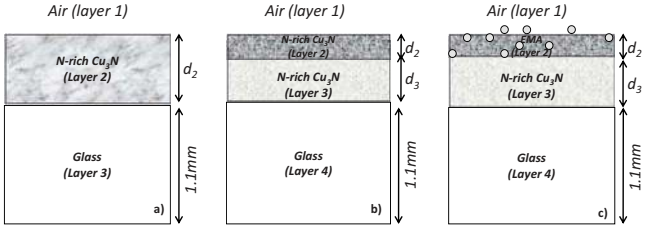

FIG. 7. (Color online) Schematic representation of the proposed layer models for (a) as-deposited and annealed (b) at 100 °C and (c) 300 °C films.

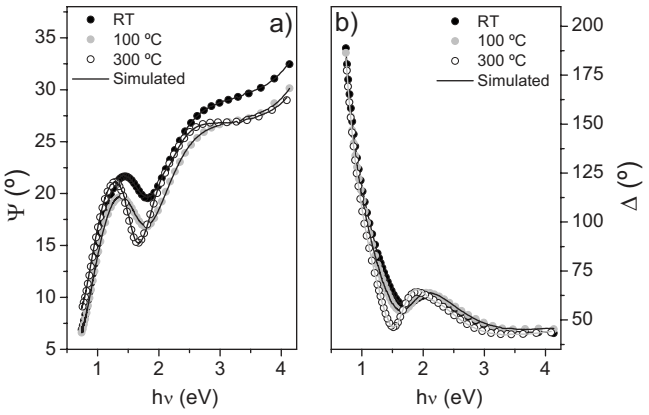

FIG. 8. Measured SE parameters Ψ [Fig. 8(a)] and Δ [Fig. 8(b)] for an as-deposited film (black dots), annealed at 100 °C (gray dots) and at 300 °C (open dots). Simulated SE parameters (black line), for the simulations the schematic model described in Fig. 7 was assumed.

For none of the annealed films the SE spectra can be fitted in the frame of this three-layer model but a more sophisticated approach is needed. In accordance with XRD and IBA data a four-layer model as illustrated in Fig. 7(b) has been tried. It consists on air (layer 1), a Cu_3N intrinsic semiconducting plus a certain Drude contribution film with thickness d_2 (layer 2), an intrinsic semiconductor Cu_3N film with a different (lower than that of layer 2) Drude contribution and thickness d_3 (layer 3) and the glass substrate (layer 4). The model parameters are listed in Table I. This four layers model provides a good fit for films heated below 300 °C. The needed for two N-rich Cu_3N layers with different density of free carriers, thus with different nitrogen concentration, confirms the nitrogen migration from the bulk to the film surface. Moreover, it is worthwhile to mention that, as shown in Table I, the calculated best-fit thickness of the N-rich Cu_3N layers that give rise to the best fit is in good agreement with the percentage of the chemical phases estimated from Rietveld refinements for all annealed films.

For the films heated at 300 °C the agreement between experimental and calculated (on the basis of the previously described four-layer model) SE data is significantly worse than that obtained for films annealed at lower temperatures. This is not surprising since the presence of bubbles (observed by AFM) has not been considered in the model. In this particular case a good fit is achieved by using the previous four layer model but substituting the layer 2 by an effective medium [Fig. 7(c)] consisting of vacancies which may represent bubbles imbibed in the N-rich Cu_3N film and layer 3 by an intrinsic Cu_3N semiconductor.

All these results evidence that optical SE data provide a reasonable support for the N migration from the bulk to the film surface.

IV. SUMMARY AND CONCLUSIONS

The annealing-induced changes in the atomic composition and in the physical properties of N-rich Cu_3N thin films have been investigated by means of IBA, XRD, AFM and SE techniques.

Concerning the thermal stability of the films it is concluded that annealing promotes nitrogen to move from the bulk to the film surface at temperatures as low as 100 °C. Nitrogen migration originates the formation of two phases with different atomic percentages of nitrogen, lattice parameter and crystallographic orientations, but with the same crystal structure. The reason for the formation of these particular phases might be related with the thermodynamically stability of the system. Nevertheless, their origin should be further investigated. From the macroscopic point of view nitrogen migration gives rise to remarkable changes in the optical properties of the films. This fact and the low temperature at which nitrogen start to migrate are very relevant data which have severe implications in the development of Cu_3N-based functional devices.

The observed Vegard-type correlation between lattice parameter and the concentration of nitrogen brings some light into the long-standing problem of extra nitrogen location, suggesting that the excess nitrogen incorporates into the anti-ReO_3 crystal lattice structure (possibly occupying body-centered interstitial positions) forming an interstitial solid solution.

In conclusion, all gathered data provide a detailed picture of thermal decomposition processes of copper nitrides and contribute to clarify the location of the excess nitrogen into the film structure.

ACKNOWLEDGMENTS

The authors want to thank to Dr. Rainer Groetzschel, Dr. D. Güttler for some NRA measurements, and to Dr. F. Agulló-Rueda for the Raman measurements and for the very helpful discussions. R.G.A and N.G. acknowledge to the M.E.C and C.S.I.C., Juan de la Cierva, and M.C.Y.T. (Grant No. FIS 2008-01431) for the financial support. The NRA measurements were supported by the EU- "Research Infrastructures Transnational Access" program AIM "Center for Application of Ion Beams in Materials Research" under EC Contract No. 025646.

[1]S. Terada, H. Tanaka, and K. Kubota, J. Cryst. Growth **94**, 567 (1989).
[2]C. Navío, M. J. Capitán, J. Álvarez, F. Yndurain, and R. Miranda, Phys. Rev. B **76**, 085105 (2007).
[3]T. Törndahl, Ph.D. thesis.
[4]C. Gallardo-Vega and W. de la Cruz, Appl. Surf. Sci. **252**, 8001 (2006).
[5]G. Soto, J. A. Diaz, and W. de la Cruz, Mater. Lett. **57**, 4130 (2003).
[6]N. Gordillo, R. Gonzalez-Arrabal, M. S. Martin-Gonzalez, J. Olivares, A. Rivera, F. Briones, F. Agulló-López, and D. O. Boerma, J. Cryst. Growth **310**, 4362 (2008).
[7]K. Venkata Subba Reddy, A. Sivasankar Reddy, P. Sreedhara Reddy, and S. Uthanna, J. Mater. Sci.: Mater. Electron. **18**, 1003 (2007).
[8]T. Maruyama and T. Morishita, J. Appl. Phys. **78**, 4104 (1995).
[9]K. J. Kim, J. H. Kim, and J. H. Kang, J. Cryst. Growth **222**, 767 (2001).
[10]Y. Du, A. L. Ji, L. B. Ma, Y. Q. Wang, and Z. X. Cao, J. Cryst. Growth **280**, 490 (2005).
[11]Z. Q. Liu, W. J. Wang, T. M. Wang, S. Chao, and S. K. Zheng, Thin Solid Films **325**, 55 (1998).
[12]L. Maya, J. Vac. Sci. Technol. A **11**, 604 (1993).
[13]T. Nosaka, M. Yoshitake, A. Okamoto, S. Ogawa, and Y. Nakayama, Thin Solid Films **348**, 8 (1999).
[14]G. H. Yue, P. X. Yan, J. Z. Liu, M. X. Wang, M. Li, and X. M. Yuan, J. Appl. Phys. **98**, 103506 (2005).
[15]T. Nosaka, M. Yoshikate, A. Okamoto, S. Ogawa, and Y. Nakayama, Appl. Surf. Sci. **169–170**, 258 (2001).
[16]D. M. Borsa, S. Grachev, C. Presura, and D. O. Boerma, Appl. Phys. Lett.

80, 1823 (2002).
[17]X.-D. Ma, D. I. Bazhanov, O. Fruchart, F. Yildiz, T. Yokoyama, M. Przybylski, V. S. Stepanyuk, W. Hergert, and M. Kirschner, Phys. Rev. Lett. **102**, 205503 (2009).
[18]D. M. Borsa, Ph.D. thesis, Material Science Centre, University of Groningen, Netherlands, 2004.
[19]J. M. D. Coey, J. Magn. Magn. Mater. **200**, 405 (1999).
[20]S. K. Shrestha, H. Timmers, K. S. A. Scott Butcher, and M. Wintrebert-Fouquet, Curr. Appl. Phys. **4**, 237 (2004).
[21]I. Fernández-Martinez, M. S. Martín-González, R. González-Arrabal, R. Álvarez, F. Briones, and J. L. Costa-Krämer, J. Magn. Magn. Mater. **320**, 68 (2008).
[22]S. Ghosh, F. Singh, D. Choudhary, D. K. Avasthi, V. Ganesan, P. Shah, and A. Gupta, Surf. Coat. Technol. **142–144**, 1034 (2001).
[23]Y. Du, R. Huang, R. Song, L. B. Ma, C. Liu, C. R. Li, and Z. Cao, J. Mater. Res. **22**, 3052 (2007).
[24]D. J. W. Mous, A. Gottdang, and R. G. Haitsma, Nucl. Instrum. Methods Phys. Res. B **109**, 177 (2001).
[25]D. J. W. Mous, A. Gottdang, R. G. Haitsma, G. García-López, A. Climent-Font, F. Agulló-López, and D. Boerma, Inst. Phys. Conf. Ser. **680**, 999 (2003).
[26]E. Andrzejewska, R. Gonzalez-Arrabal, D. Borsa, and D. O. Boerma, Nucl. Instrum. Methods Phys. Res. B **249**, 838 (2006).
[27]J. R. Tesmer and M. Nastasi, *Handbook of Modern Ion Beam Materials Analysis*, MRS Symposia Proceedings No. 980 (Materials Research Society, Pittsburgh, 1995), p. 158.
[28]A. C. Larson and R. B. Von Dreele, "General Structure Analysis System (GSAS)," Los Alamos National Laboratory Report No. LAUR 86–748, 2004.
[29]I. Horcas, R. Fernández, J. M. Rodríguez, J. Colchero, J. Gómez-Herrero, and M. Baro, Rev. Sci. Instrum. **78**, 013705 (2007).
[30]V. I. Soroka, M. V. Artsimovich, I. Yu Lobach, I. F. Mogilnik, V. N. Pavlovich, V. V. Tokarevsky, E. M. Kudriavtsev, and B. N. Romanjuk, Nucl. Instrum. Methods Phys. Res. B **83**, 311 (1993).
[31]JCPDS File No. 471088.
[32]C.-F. Huang, B.-Y. Tsui, and C.-H. Lu, Jpn. J. Appl. Phys., Part 1 **47**, 872 (2008).
[33]Z. F. Hou, Solid State Sci. **10**, 1651 (2008).
[34]J. Blucher and K. Bang, Mater. Sci. Eng., A **117**, L1 (1989).
[35]N. Gordillo, R. Gonzalez-Arrabal, A. Alvarez-Herrero, and F. Agulló-López, J. Phys. D **42**, 165101 (2009).
[36]JCPDS File No. 040836.
[37]JCPDS File No. 471072.